A Statistical Approach to Mitigating Persistent Clutter in Radar Reflectivity Data

Valliappa Lakshmanan[1,2], Jian Zhang[2], Kurt Hondl[2], Carrie Langston[1,2]

Abstract

Although there are several effective signal processing methods for identifying and removing radar echoes due to ground clutter, the need to mitigate persistent clutter in radar moment data still exists if such techniques were not applied during data collection and the time series data are not available.

A statistical approach to creating a clutter map from "found data" i.e. data not specifically collected in clear air is described in this paper. Different methods of mitigating ground clutter are then compared using an information theory statistical approach and the best mitigation approach chosen.

The technique described in this paper allows for the mitigation of persistent ground clutter returns in archived data where signal processing techniques have not been applied or have been conservatively applied. It is also helpful for correcting mobile radar data where the creation of a clear-air clutter map is impractical. Accordingly, the technique is demonstrated in each of the above situations.

I. Introduction

Reflectivity data from ground-based weather radars can be contaminated with echoes from ground-clutter targets such as trees, mountains and buildings. Several techniques exist for identifying and removing ground clutter from in-phase and quadrature-phase data at the radar [1], [2]. These techniques are carried out operationally on most weather radar systems, and the received moment data typically have been corrected using these time series data filters. However, the filters require parameter settings, and in some instances the parameters are set conservatively to avoid removing potentially good data.

Consequently, the signal processing removal of ground clutter echo has to be followed with some processing of the reflectivity moment data to remove left over ground clutter targets. A preliminary stage of quality control for many algorithms, for example the precipitation algorithm of [3], is to remove echoes at locations where the radar beam would be blocked under standard atmospheric conditions.

While correction for beam blockage due to terrain can correct for ground clutter due to mountains, the terrain maps do not include the height of buildings or tree cover at every grid point. Also, construction activity, plant growth and the presence or absence of leaves on deciduous land cover can cause annual and seasonal changes in the locations of ground clutter targets. Thus, in addition to the terrain map, a map of ground clutter locations is often maintained by the radar station. This Clutter Residue Editing Map (CREM) or "bypass" map is created by running the radar on a clear-air day and noting the locations of strong echoes at different elevations [4]. Echoes at these known clutter locations can be deleted or interpolated over before being presented to users and automated data processing algorithms. Currently the NEXRAD system also supports the application of a dynamic Clutter Mitigation Decision (CMD; [5]).

Automated techniques also exist to process the 2D reflectivity data to identify ground clutter based on the idea that ground clutter tends to be stationary, have a narrow spectrum width [6] and little vertical extent [7]. Such features can be used as inputs to a neural network [8] and used to discriminate between meteorological and non-meteorological echoes.

Corresponding author: V Lakshmanan, University of Oklahoma, Norman OK lakshman@ou.edu [1] Cooperative Institute of Mesoscale Meteorological Studies, University of Oklahoma [2] National Severe Storms Laboratory, Norman, OK

However, these data processing techniques tend to be imperfect and, as shown in [9], even a 99% accuracy rate on reflectivity pixel data can result in a bad three-hour accumulation of precipitation 30% of the time. The solution proposed by [9] was to average the classification result within contiguous reflectivity objects, to dramatically increase the classification accuracy to 99.97% on reflectivity echoes above 30 dBZ. However, averaging the classification result within contiguous areas of reflectivity is subject to a systematic problem – it fails when there is ground clutter embedded inside or connected to an area of precipitation.

In this paper, we present a novel approach to pre-filter the reflectivity moment data before presenting it to an automated quality control algorithm that averages the classification result within contiguous reflectivity objects. In the pre-filtered data, clutter pixels will have their values replaced with a better estimate of the "true" reflectivity.

Contamination of radar data by ground clutter poses a problem to precipitation algorithms [3]. The problem is less severe in NEXRAD data where the time series clutter filtering parameters are aggressive and bypass maps well maintained, leaving little in the way of ground clutter contamination. It is, however, a problem in the case of operational data from Canada where the time series filtering is more conservative and bypass maps not current. [1] It is also a problem in data from mobile radars where the atmospheric conditions may not be right to collect and create a bypass map or no time is available to create the bypass map. Thus, this paper explores a method of applying a statistical clutter correction method for mobile radar case studies and real-time processing of radar data contaminated by significant persistent clutter.

It should be noted that the technique of this paper seeks to mitigate only persistent ground clutter, not all forms of non-meteorological echoes. For example, anomalous propagation or AP is a separate problem that we do not address here since AP is handled well by existing automated quality control techniques. The clutter mitigation technique presented in this paper is followed by an automated quality control technique [9], [12] that averages classification results in contiguous areas of reflectivity in order to obtain misclassification errors on the order of 0.01%. The key purpose of the clutter mitigation approach of this paper is to correct for clutter pixels that are embedded within valid echoes and, therefore, pose problems when averaging classification results within contiguous areas of reflectivity.

The rest of this paper is organized as follows. We describe how to identify locations of persistent clutter in Section II given a dataset that was not specifically collected in clear air to identify clutter i.e. given a dataset collected "in weather", but that happens to include ground clutter pixels. The reflectivity value at clutter points can be corrected in one of several ways, described in Section III. In Section III, we also describe a statistical test that can be used to choose the best available correction technique for that dataset. The identification and correction techniques are demonstrated on Canadian, mobile radar, NEXRAD and simulated data in Section IV.

II. Identifying Persistent Clutter

In this paper, we are concerned with identifying and removing persistent clutter i.e. radar echoes that do not move at all from a data set consisting of several hours of radar reflectivity data.

If this were a supervised machine learning problem i.e. if we had, say, rainfall information or expert classifications, then reflectivity and rainfall at various pixel locations over a long enough period could be used to classify the pixels into clutter and no-clutter using a neural

[1]Although a "Corrected Reflectivity" product is also produced operationally in Canada, that product is available only for specific Doppler volumes and only at the lowest levels. Since we needed the Canadian data to incorporate it into a real time rapidly updating 3D mosaic [10], [11], we needed to mitigate clutter in all the reflectivity scans.

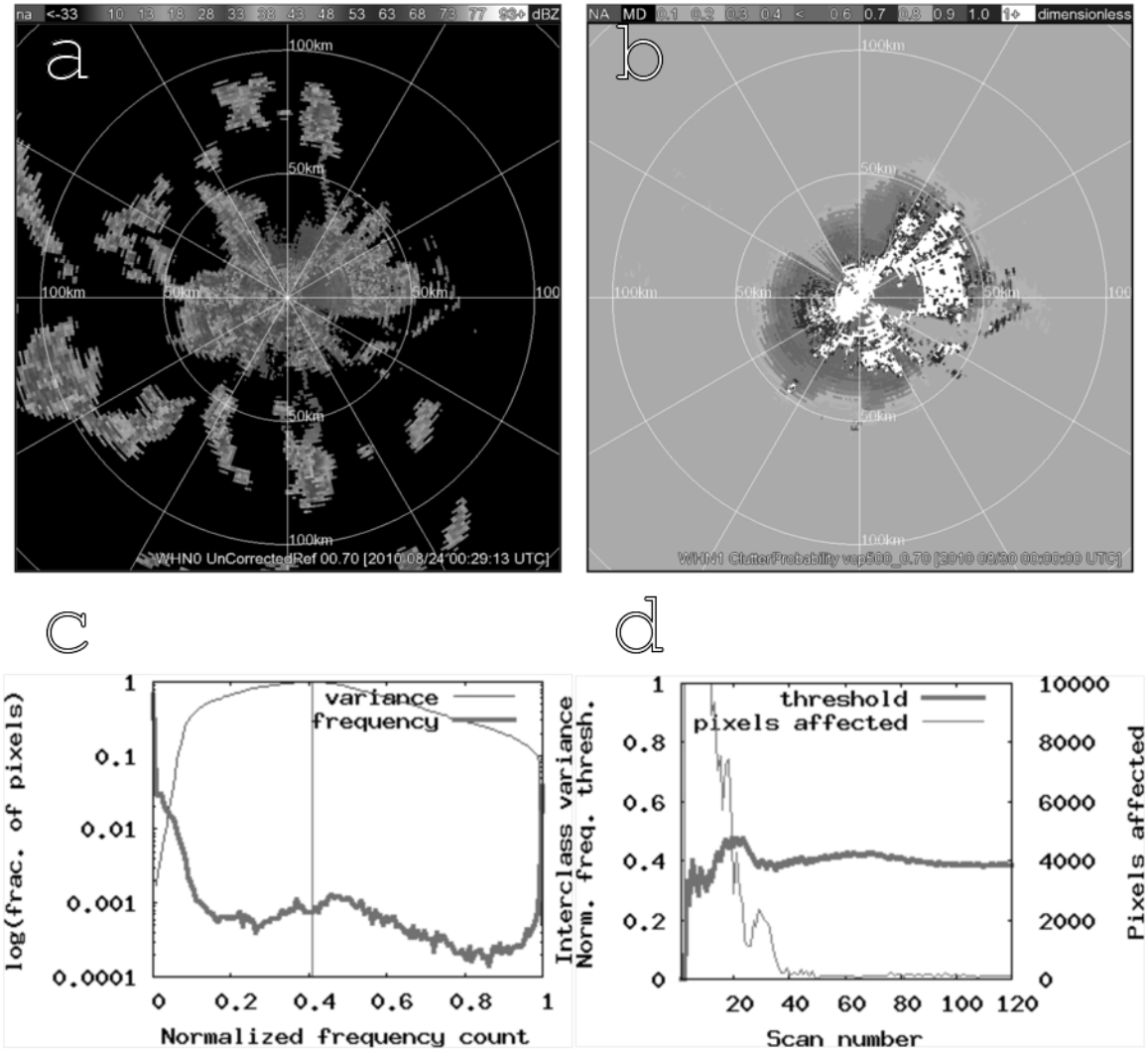

Fig. 1. The process of identifying persistent clutter demonstrated on a data from the Jimmy Lake, Alberta (WHN) radar on Aug. 24, 2010. (a) An example of data from this radar. (b) Normalized frequency count of how often a pixel's reflectivity value is greater than 0 dBZ in the dataset. (c) Histogram of normalized frequency count shown on a logarithmic scale and the inter-class variance by threshold. The vertical line is the final threshold (See Equation 1). (d) Variation of threshold and number of pixels affected by the change in threshold as the number of 0.70-degree elevation scans in the dataset is increased.

network or decision tree. Such a training dataset of rainfall is impractical since rain gage networks tend to be geographically much sparser than radar range bins.

The underlying idea is that if radar echoes move, then in a long-enough sample, any non-clutter point will have reflectivity below, say, 0 dBZ at least some of the time. How long of a time period needs to be considered before the results are reliable? What fraction of the scans should the echo be present in before it is considered "persistent"? Both of these questions can be answered statistically from internal measures of the dataset itself.

The first step is to walk through the dataset and start to accumulate a frequency count of the number of times that a pixel's reflectivity value exceeds 0 dBZ. Because ground clutter characteristics change with radar pulse length, scanning rate and elevation, this accumulation would have to be by Volume Coverage Pattern (VCP) and elevation. The resulting frequency

count can then be normalized by the number of scans to yield an image as shown in Figure 1b. This is the fraction of time that a pixel has echo. If a long enough time period is considered, then high values of this fraction indicate persistent clutter and low values indicate pixels where echoes are not persistent.

A histogram of values that the fraction takes is plotted for each elevation at each VCP as shown in Figure 1c. In that histogram, the x-axis is a fraction between 0 and 1. The right extreme (x=1) represents all of the radar scans at a particular elevation and VCP in the dataset while the left extreme (x=0) represents none of those scans. The y-axis gives the fraction of pixels which have reflectivity greater than 0 dBZ. Thus, towards the left of the histogram are the pixels for which there is rarely any reflectivity data above 0 dBZ i.e. the non-clutter pixels. The peak on the right corresponds to the clutter pixels which nearly always have a reflectivity value greater than 0 dBZ. The question of classifying pixels into clutter and no-clutter becomes one of finding an optimal threshold to best separate the histogram into two classes. Note that the histogram in Figure 1c is on a log-scale: the two peaks at the edges are many factors of magnitude larger than the values in between. If drawn on a linear scale, the values near x=0 and x=1 would dominate the plot to an extent that y-values in the middle would appear to be zero.

Threshold selection from a gray-level histogram is a well-studied problem in information theory [13]. Because the histograms for our clutter vs. no-clutter problem tend to be bimodal (well-separated into two classes with well-defined peaks), we employ a method devised by Otsu [14] that maximizes the inter-class variance by finding the threshold k at which

$$\sigma_k^2 = \frac{(\mu_T \omega_k - \mu_k)^2}{\omega_k(1-\omega_k)} \tag{1}$$

is maximum. In Equation 1, ω_k and μ_k are the zeroth and first order cumulative moments of the histogram up to the k^{th} level i.e.:

$$\omega_k = \sum_{i=1}^{k} p_i \tag{2}$$

and

$$\mu_k = \sum_{i=1}^{k} i p_i \tag{3}$$

while T is the maximum possible value of the threshold k, which in our case would be the number of radar scans at the elevation and VCP in the dataset over which the histogram was computed. The p_is are the frequencies in the histogram.

If the clutter mitigation approach will be followed by a more general purpose automated quality-control technique such as [9], [12], one might wish to be more conservative in identifying pixels as clutter since any remaining clutter pixels could be handled in later stages. To be more conservative in identifying pixels as clutter, it is possible to choose the final threshold to be between k^*, the threshold at which Equation 1 is maximized, and T, the maximum possible threshold. In this paper, we will simply use k^*, variance-optimizing threshold, as the final threshold. The variation of σ_k^2 with k, as well as the final threshold k^*, is shown in Figure 1c.

One issue that we have to address when defining clutter pixels as pixels that tend to always have reflectivity value greater than zero is of how to determine if our dataset is large enough. On a small dataset, the presence of a large storm will cause a number of pixels to always have high reflectivity values even though they are not clutter. In order to assure ourselves that

the dataset is of sufficient size, we can examine the variation of the threshold k^* as the data from a new scan is incorporated and examine how many pixels change classification from clutter to non-clutter or vice-versa. When the threshold converges and the number of pixels is below some pre-determined (subjective) threshold, we have enough data. The variation of the threshold and the number of pixels affected by the change in threshold as the number of scans is increased in shown in Figure 1d. On this particular dataset, it appears that about 50 reflectivity scans suffice to form a relatively consistent clutter map. The number of scans required varies from case to case (depending on the season, type of weather etc.), so users of the technique described in this paper should ensure that their dataset is long enough.

Once the threshold k^* has been determined, any pixels in the frequency image (See Figure 1b for an example) that have reflectivity greater than 0 dBZ in more than k^* scans are classified as clutter pixels.

III. Correction of radar reflectivity

For correcting the clutter, it might be necessary to determine the reflectivity value associated with a clutter pixel. For example, we might want to correct the reflectivity value at a pixel using the reflectivity associated with clutter. The minimum clutter reflectivity value associated with a clutter pixel is the $100(1 - n/T)$th percentile of the reflectivity values at the pixel over the dataset where n is the frequency count at that pixel i.e. the number of scans that the reflectivity is greater than 0 dBZ. Thus, the median clutter reflectivity value associated with a clutter pixel is the $50(1 - n/T)$th percentile of the reflectivity values at the pixel over the complete dataset. This was defined as the clutter reflectivity value associated with that clutter pixel.

The following strategies were tested to correct the radar reflectivity at clutter pixels:

1. **Retain**: The clutter pixel was not corrected. Instead, its reflectivity value was retained. However, the rest of the automated quality control of [9] was applied, so in effect, this is a test of whether the clutter mitigation helps or hinders overall quality.
2. **Delete**: The clutter pixel was simply set to be unavailable. This results in holes in the resulting reflectivity field but serves as another baseline of clutter correction performance.
3. **Interpolate along radials**: Clutter pixels were filled in with dBZ values interpolated from their nearest non-clutter neighbors along the radial. If only one non-clutter neighbor existed (as with clutter pixels abutting the radar), then the pixel was set to missing if closer to the boundary than to the non-clutter neighbor. Interpolation was not carried out for longer than 3 gates. If the distance of a clutter pixel from a non-clutter gate was more than 3 pixels, then the Subtract dBZ strategy (see below) was carried out. We chose to interpolate in dBZ rather than in Z because smoothing and other image processing of weather radar reflectivity fields e.g. [15], [16], [17], [18], [19], [7], [6] has traditionally been carried out in dBZ. This is because Z is not conducive to arithmetic operations: the difference between 52 dBZ and 53 dBZ if computed on their corresponding Z values is 46 dBZ, for example. The choice of 3 gates was heuristic and used to safeguard against interpolating across dramatically different storm-scale phenomena.
4. **Interpolate in 2D**: As with the previous, except that the interpolation was bi-linear in both azimuth and range.
5. **Subtract Z**: The reflectivity factor (Z) corresponding to the clutter was subtracted from the Z received at the pixel to yield the corrected value. This is commonly argued to be the "right" thing to do, but it performs poorly in practice. We include this strategy in order to demonstrate this.
6. **Subtract dBZ**: As with the previous, except that the subtraction was carried out in logarithmic space. This appears theoretically unsound but it performs better in practice

TABLE I

USING THE D-STATISTIC TO EVALUATE THE VARIOUS MITIGATION STRATEGIES ON DATA FROM JIMMY LAKE, ALBERTA. THE BEST STRATEGY ON THIS DATA SET IS TO SIMPLY DELETE THE DATA AT CLUTTER PIXELS. THE SECOND BEST IS TO INTERPOLATE BI-LINEARLY.

Strategy	d-statistic
Delete	0.24
InterpolateBilinear	0.35
InterpolateRadial	0.37
Retain	0.61
SubtractDbz	0.39
SubtractPower	0.58

because of the numerical properties of the Z and dBZ scales.

Which of these techniques yields the best performance? Because there is no true reflectivity value available against which to compare the corrected value, we use internal measures on the data to choose the best correction strategy, since different datasets (indeed different VCPs within the same dataset) might call for different correction strategies.

The distribution over the entire dataset of corrected reflectivity values ought to be similar to the distribution of reflectivity values at non-clutter pixels. The comparison of the two distributions is carried out using the non-parametric Kolmogorov-Smirnov (KS) test [20]. The KS test finds the maximum absolute distance ("d-statistic") between the cumulative probability distribution (CDF) of corrected reflectivity and the CDF of good reflectivity data. We can then choose the strategy whose d-statistic is smallest. This is shown for Canadian data in Figure 2i and in Table I. In that particular case, deleting clutter values yields corrected reflectivity values over the whole dataset whose CDF is closest to that of the uncorrected reflectivity values at non-clutter locations.

IV. RESULTS AND DISCUSSION

A. Canadian data

The clutter mitigation technique described in this paper was carried out on data collected from the Jimmy Lake, Alberta (WHN) radar on Aug. 24, 2010 (from 00:00Z to 23:59Z). A 0.7 degree scan from this radar on that day is shown in Figure 2. There was mild precipitation through out the day, but the resulting clutter map (top row of Figure 2) was very similar to the clutter map extracted on a clear-air day. The different correction strategies were carried out, and based on the KS test, the best correction strategy is to carry out bi-linear interpolation. Figure 2i shows the impact of the different correction strategies as evaluated by the K-S test. The closer the cumulative fraction is to the "Good" curve, the better the mitigation technique. It is also clear that subtracting Z is a particularly poor strategy. The best strategy for this case is to simply delete clutter pixels. The other mitigation strategies are all bunched together but are worse than the "Delete" strategy. The d-statistic from the Kolmogorov-Smirnov test is shown in Table I.

B. Need for Doppler velocity

One concern with a statistical technique such as this is the question of how it behaves under inappropriate use. For example, what would happen if the technique were applied to extremely small amounts of good data with little or no clutter? For instance, the clutter map for the Oklahoma City, OK radar (KTLX) shown in Figure 3 was generated from just 4 hours of data. Thus, if the technique of this paper is applied to small datasets of fast

moving storms, biological echoes may get misidentified as clutter, but the storm data itself tends to not be affected. Areas that happened to have been covered by a storm system over the 4 hours of the dataset may also be misidentified as clutter. To avoid triggering clutter removal due to biological echoes, we recommend that the technique of this paper be applied on at least 24 hours of data, over a complete diurnal cycle. In summer, some WSR-88Ds have near-range biological echoes almost continuously, so even a diurnal dataset may not be enough.

If the clutter map is created over a smallish dataset that can be impacted by biological echoes, some clutter mitigation strategies are more dangerous than others. If using an interpolation strategy, the entire area of biological echo will be removed and interpolated over, a process that will remove all the echoes near the radar in the case of the data shown in Figure 3. To safeguard against this and related problems of smoothing across different storm-scale phenomena, we limit interpolation to just 3 gates. On biological echoes, the subtraction strategies tend to be safer because the clutter reflectivity is low enough that the correction causes little impact.

A similar problem happens when this technique is applied to slow-moving, widespread meteorological phenomena such as lake-effect snow (see middle row of Figure 3). Although the clutter map for the Buffalo radar was derived from 24 hours of data, that period happens to include an episode of lake-effect snow, which moves very little. Thus, many pixels always have reflectivity greater than zero and are wrongly identified as persistent clutter.

Both biological echoes and slow moving storm systems can be handled if Doppler velocity data is available. In that case, we treat a pixel as possibly clutter only if it has both reflectivity greater than 0 dBZ and near-zero velocity (defined in this paper as absolute value less than 0.5 m/s). As shown in the bottom row of Figure 3, neither biological echoes nor slow-moving systems pose a problem if Doppler velocity data are used in conjunction with reflectivity data to identify persistent clutter. If Doppler velocity are also used, then the dataset needs only to be long enough for the wind direction to change, to avoid misidentifying gates with wind velocity tangential to the radar beam as clutter.

C. Nomadic applications

Mitigating clutter from nomadic applications of mobile radar data has typically been performed manually by editing the data before it is analyzed or assimilated into numerical models. Because this is a time-consuming and labor-intensive process, it takes many months after data collection before case studies with that data can be performed.

Because nomadic mobile radars are moved to their positions minutes before data collection on a storm starts, the option of running a clear-air scan to create a map of ground clutter does not exist. The statistical technique proposed in this paper can be used to automatically create a map of ground clutter that can then be used to mitigate ground clutter. One potential issue is that the data lengths are rarely very long. Because the range of a mobile radar is usually quite limited, the radars have to be moved quite often. Of course, once a radar is moved, the clutter map will have to change. Because the data lengths are short, this technique should be applied only if Doppler velocity data is available so that a pixel is considered to be clutter only if it has persistently high reflectivity and near-zero velocity (See Section IV-B).

We carried out the statistical clutter mitigation technique of this paper on data collected by NOXP, a mobile X-band dual-polarimetric Doppler radar built and operated by the National Severe Storms Laboratory (NSSL). The data were collected during the Verification of the Origins of Rotation in Tornadoes Experiment 2 (VORTEX2), a nomadic field program to study tornadoes. The lowest scan of reflectivity collected on May 26, 2010 is shown in

Figure 4. The data are contaminated by ground clutter close to the radar. The correction performed by the signal processor, shown in Figure 4b, did not remove any of the ground clutter. The clutter reflectivity derived from just 90 minutes of data (from 22:12 UTC to 23:48 UTC) was accurate enough to be able to remove the persistent ground clutter, as seen in Figure 4d. It is conceivable that this technique could be used for even shorter episodes of data collection. We expect that even smaller datasets (30 minutes, for example) would suffice as long as the wind direction is variable within the collection period (so that gates where the wind direction is tangential to the radar beam are not misidentified as clutter).

Interpolating along radials was the best clutter mitigation strategy according to the KS-test and consequently, Figure 4d shows the cleaned-up image where the clutter pixels were interpolated over in one dimension. However, the use of the KS test to choose the best mitigation strategy is not justifiable in the context of a nomadic field experiment such as VORTEX2. Recall that the motivating factor behind the KS test was that the distribution of reflectivity values at clutter and non-clutter pixels ought to be similar. This is reasonable for fixed radars where there is nothing special about any particular location – over a long enough period of time, any pixel should experience the same weather as other pixels within the domain. However, mobile radars are actively moved in order that the operators can remain outside the storm, but close enough to it. Thus, the motivating assumption behind the KS test does not hold. Indeed, since ground clutter tends to be near the radar and the radar tends to be outside the storm, ground clutter points are more likely to be in clear-air. Thus, it could be argued that the "Delete" strategy is more appropriate for mitigating ground clutter in mobile radar applications.

D. Simulation of clutter

While internal statistical measures are well-and-good, a question that arises is whether clutter removal of the sort proposed in this paper is truly safe. As alluded to earlier, there is no ground truth to the radar observation and therefore it is not possible to verify that a pixel being removed is truly clutter. In particular, it is impossible to verify what the "true" reflectivity would have been absent the ground clutter target. Earlier studies of quality control have used alternate radars [6], rain gages [8] or human verification [9] to evaluate the skill of automated quality control. Human verification is time consuming and subjective. Alternate radars are not available outside of experimental settings (and very costly to deploy). Rain gage-based verification is problematic because such verification relies on Z-R relationships that are themselves heuristic.

Because the purpose of the technique of this paper is only to remove persistent ground clutter, it is possible to side-step the problem of unknowable truth by simulating ground clutter targets, adding them to valid reflectivity data probabilistically and then evaluating how well the technique does at mitigating the effects of the added noise. Because the true reflectivities (before noisy clutter targets were added) are known, it is possible to evaluate the Root Mean Square (RMS) error between the mitigated field and the true reflectivity field.

We took the data collected by the Oklahoma City NEXRAD on May 20, 2001 between 16:30Z and 23:59Z and added ground clutter targets to it under three clutter scenarios: the probability of clutter p of 0.01, 0.05 and 0.1 (See Figure 5). At each scenario, p of the range gates in the image up to a maximum range of 200 km. [2] were randomly chosen to be gates with persistent clutter. At each of these ground clutter pixels, the nominal clutter reflectivity was randomly chosen from a normal distribution centered at 50 dBZ and with a standard

[2]This range restriction is because Doppler velocity data on the NEXRAD system is not available to the full range of the reflectivity data.

deviation of 10 dBZ. The nominal clutter reflectivity value was truncated at 10 dBZ i.e. if the randomly obtained clutter value was less than 10 dBZ, it was set to be 10 dBZ. Each of the clutter pixels was simulated to be clutter p of the time. The actual clutter reflectivity at each pixel varied with time and was chosen from a normal distribution centered at the nominal clutter reflectivity at that pixel and with a standard deviation of 3 dBZ. Whenever a pixel was simulated as clutter, the Doppler velocity value at that pixel at the corresponding time was set to be zero. The reflectivity in the simulated field was set to be the sum of the original power collected by the radar on May 20, 2001 and the simulated clutter power. It is this simulated clutter field that was presented to the clutter mitigation technique of this paper.

An example of the lowest scan of reflectivity is shown in Figure 5. While the speckle can be removed by existing quality control techniques, clutter embedded within valid echoes is harder to remove. All of the clutter mitigation strategies work well at mitigating the impact of the clutter but the "Delete" and "SubtractPower" strategies are aesthetically not pleasing. The "Delete" strategy results in holes where clutter was identified, while the "SubtractPower" does not continues to have high-reflectivity speckle that is an improvement over the uncorrected data, but not dramatically so. The reason for this is easy to see: because the simulated clutter reflectivity varies by $+/-3$ dBZ (variation of this order is typical over the course of a long-time archive), correcting clutter by subtracting Z (as opposed to subtracting dBZ) is typically not enough. This can be verified numerically: if the median reflectivity of clutter is 52 dBZ and at some point that pixel has a reflectivity of 53 dBZ, the corresponding Z values are 158489 and 199526, resulting in the difference in Z equivalent to 46 dBZ. Since we are computing this difference from the median and because clutter reflectivity values tend to be high, the correction will not be enough in half the cases.

The skill of the algorithm at identifying persistent clutter using the method of thresholding the clutter probability at a threshold determined using Otsu's method is shown in Table II. As can be seen, the algorithm is quite conservative, with no false alarms (i.e. no good data identified as clutter) in any of the simulations. In spite of this, the classification accuracy is quite high. At such low probabilities, however, it is better to look at the probability at which clutter pixels are detected (POD), and this is around 60%. By choosing thresholds lower than those suggested by Otsu's method, it is possible to raise the POD but at the expense of sometimes correcting valid data values.

The RMS errors of the various mitigation strategies at different clutter probabilities are shown in Table III. The reported error bars are one standard deviation. The "KSTest" strategy is the optimal strategy as selected by the Kolmogorov-Smirnov test, and is a mix of different strategies at different VCPs. The "Retain" field is the field without clutter mitigation but with automated quality control, so that most of the speckle clutter is removed, but clutter embedded within storm echoes is not. The "Simulated" field is the field without any quality control applied – as expected, the RMS error increases as the probability of clutter goes up and when nearly 10% of data values are clutter, there is very little a clutter mitigation strategy can do. But even then, the clutter mitigation strategies do reduce the error by a statistically significant amount.

The differences in RMS error between the the different strategies (other than "Retain" which is expected to do poorly) do not rise above statistical significance. The problems with "Delete" and "Subtract Power" are mostly aesthetic – statistically, they are just as good as any of the other clutter mitigation strategies. Any of these clutter mitigation strategies are better than not identifying clutter ("Retain") and this difference is statistically significant. Because clutter was simulated by adding Zs, the "Subtract Power" strategy should be expected to perform well, but the incorporation of noise in the added clutter

TABLE II

SKILL OF ALGORITHM AT IDENTIFYING SIMULATED CLUTTER PIXELS AT VARIOUS PROBABILITIES OF CLUTTER. A "HIT" IS DEFINED AS A CLUTTER PIXEL CORRECTLY IDENTIFIED AS CLUTTER AND THE POD IS THE PROBABILITY THAT A SIMULATED CLUTTER PIXEL IS CORRECTLY IDENTIFIED AS CLUTTER. THE RMSE IS THE ROOT MEAN SQUARE ERROR OF THE CLUTTER REFLECTIVITY ESTIMATE AT CORRECTLY IDENTIFIED CLUTTER PIXELS.

p	Null	Hit	FA	Miss	Accuracy	POD	RMSE (dBZ)
0.01	82397	460	0	303	0.996	0.60	1.16
0.05	79539	2383	0	1238	0.985	0.66	1.16
0.1	75890	4731	0	2539	0.969	0.66	1.20

TABLE III

RMS ERROR IN DBZ WHEN VARIOUS MITIGATION STRATEGIES WERE APPLIED TO DATASET WITH SIMULATED CLUTTER.

Strategy	RMS Error (dBZ)		
	$p = 0.01$	$p = 0.05$	$p = 0.1$
Simulated	5.67 +/- 2.37	11.43 +/- 3.33	15.50 +/- 3.82
KSTest	3.36 +/- 1.83	8.11 +/- 2.85	10.98 +/- 3.31
Retain	5.22 +/- 2.28	11.56 +/- 3.39	15.48 +/- 3.90
Delete	3.54 +/- 1.88	8.45 +/- 2.91	11.31 +/- 3.36
InterpolateRadial	3.36 +/- 1.83	8.15 +/- 2.85	11.06 +/- 3.33
InterpolateBilinear	3.35 +/- 1.83	8.11 +/- 2.85	10.98 +/- 3.31
SubtractPower	4.19 +/- 2.05	9.67 +/- 3.11	13.11 +/- 3.62
SubtractDbz	3.52 +/- 1.88	8.40 +/- 2.90	11.36 +/- 3.37

reflectivity value negates that advantage. The interpolation-based strategies, even though they "make up data", are the ones that perform best. Using the Kolmogorov-Smirnov test to identify the best strategy to use on the data did identify the interpolation strategies as the best, but selected interpolating just radials in the case of $p = 0.01$. Based on the RMSE of the interpolated data, interpolating in two dimensions would have been marginally better. Indeed, this simulation would suggest that an implementation of the technique of this paper could forgo the use of the Kolmogorov Smirnov test and arbitrarily pick any of the clutter mitigation strategies. The loss of skill by doing such an arbitrary selection appears to be not significant.

E. Real-time use

While the clutter identification technique was mainly introduced as a way to correct archived reflectivity data for ground clutter, it is fast enough to apply in real-time. Creation of a clutter map from 24 hours of NEXRAD data takes under 30 minutes on a Linux workstation with a 1 GHz CPU. Thus, it is possible to create a ground clutter map using previously collected data and then use that clutter map to correct data received in real-time. The correction itself involves just subtraction or interpolation and adds minimal overhead to an existing real-time quality control routine.

We wish to emphasize that the technique of this paper should be applied only to radar data where adequate clutter filtering has not already been carried out at the processor. Currently, a dynamic Clutter Mitigation Decision (CMD; [5]) is carried out on NEXRAD and the moments recalculated after clutter returns have been censored and so, the real-time clutter mitigation method of this paper should not be applied to real-time NEXRAD data.

It is still useful on archived NEXRAD cases where the spectral data were not filtered.

A clutter map was developed using the technique described in this paper for the Lac Castor, Quebec (WMB) radar using several days of archived data. That clutter map was then applied as part of the radar reflectivity quality control in a real-time quantitative precipitation estimation (QPE) system [21] i.e. once created from archived data, the clutter map was not updated further. Example composite reflectivity and 24-hour precipitation accumulations in the vicinity of WMB before and after the application of the clutter map are shown in Figure 6. Because this is a real-time QPE system (and because we operate only one instance of the system), the times of the two sets of images are different. However, they clearly show the impact of removing persistent clutter.

The rain gage network in Canada is sparse, but we can use station observations from Environment Canada to verify that what was removed was actually ground clutter. Bagotville, Quebec at 48.33N, 71W lies within the area where the radar data was corrected using the technique described in this paper. On Oct. 1, 2010 (before clutter removal), the daily radar QPE at Bagotville, Quebec was over 80 mm, while the surface station reported just 4 mm for that time period. On Oct. 7, 2010 (after clutter removal), the radar QPE was about 22.5 mm whereas the surface report was for 11.6 mm. After clutter mitigation, therefore, the radar-based QPE is much closer to the surface report. While this is just one instance, it serves to demonstrate that the improvement to radar-based QPE can be dramatic.

When employed in real-time, the interval at which the ground clutter maps need to be updated (once a day? once a month?) would need to be studied. One advantage of automatically creating clutter maps using a statistical technique on routinely collected data is that special clear-air scans of the radar do not need to be periodically run at all possible VCPs in order to update the clutter maps for new buildings, wind-farms, etc.

F. Summary

A fully automated, statistical clutter identification and correction technique for reflectivity moment data is described in this paper. The technique was demonstrated on several datasets that contained significant weather echoes mixed in with persistent ground clutter. It can be applied on archived datasets and used to create clutter maps to be employed in real-time. If applied to data with slow-moving, widespread meteorological systems or on short datasets, the clutter removal method described here should be applied only if Doppler velocity data are available.

Acknowledgments

Funding for Lakshmanan and Langston was provided under NOAA-OU Cooperative Agreement NA17RJ1227. The technique described in this paper has been implemented as part of the Warning Decision Support System – Integrated Information (WDSS-II; [22]) as the program w2createClutterMap. It is available for free download at http://www.wdssii.org/.

We thank Don Burgess and Dan Suppes for the NOXP data from May 26, 2010. These data were collected in part with funding provided by NOAA/Office of Oceanic and Atmospheric Research and by NSF Grant ATM-080217.

References

[1] A. Siggia and J. R. Passarelli, "Gaussian model adaptive processing (GMAP) for improved ground clutter cancellation and moment calculation," in *Proc. of 3rd European Conf. on Radar in Meteo. and Hydro.*, (Visby, Gotland, Sweden), pp. 67–73, ERAD, 2004.

[2] S. Torres and D. Zrnic, "Ground clutter canceling with a regression filter," *J. Applied Meteorology*, vol. 16, pp. 1364–72, 1999.

[3] R. Fulton, D. Breidenback, D. Miller, and T. O'Bannon, "The WSR-88D rainfall algorithm," *Weather and Forecasting*, vol. 13, pp. 377–395, 1998.

[4] FMH11C, "Doppler radar meterological observations: WSR-88D products and algorithms," Tech. Rep. FCM-H11C-2006, Federal Meteorological Handbook No. 11 Part C, Washington, DC, 2006. http://www.ofcm.gov/fmh11/fmh11.htm.

[5] J. Hubbert, M. Dixon, and C. Kessinger, "Real time clutter identification and mitigation for NEXRAD," in *23rd Int'l Conf. on Inter. Inf. Proc. Sys. (IIPS) for Meteor., Ocean., and Hydr.*, (San Antonio, TX), p. 5B.6, Amer. Meteor. Soc., 2007.

[6] C. Kessinger, S. Ellis, and J. Van Andel, "The radar echo classifier: A fuzzy logic algorithm for the WSR-88D," in *3rd Conference on Artificial Applications to the Environmental Sciences*, (Long Beach, CA), Amer. Meteor. Soc., Feb 2003.

[7] M. Steiner and J. Smith, "Use of three-dimensional reflectivity structure for automated detection and removal of non-precipitating echoes in radar data," *J. Atmos. Ocea. Tech.*, vol. 19, no. 5, pp. 673–686, 2002.

[8] M. Grecu and W. Krajewski, "An efficient methodology for detection of anamalous propagation echoes in radar reflectivity data using neural networks," *J. Atmospheric and Oceanic Tech.*, vol. 17, pp. 121–129, Feb 2000.

[9] V. Lakshmanan, A. Fritz, T. Smith, K. Hondl, and G. J. Stumpf, "An automated technique to quality control radar reflectivity data," *J. Applied Meteorology*, vol. 46, pp. 288–305, Mar 2007.

[10] J. Zhang, K. Howard, and J.J.Gourley, "Constructing three-dimensional multiple-radar reflectivity mosaics: Examples of convective storms and stratiform rain echoes," *J. Atmos. Ocean. Tech.*, vol. 22, pp. 30–42, Jan. 2005.

[11] V. Lakshmanan, T. Smith, K. Hondl, G. J. Stumpf, and A. Witt, "A real-time, three dimensional, rapidly updating, heterogeneous radar merger technique for reflectivity, velocity and derived products," *Weather and Forecasting*, vol. 21, no. 5, pp. 802–823, 2006.

[12] V. Lakshmanan, J. Zhang, and K. Howard, "A technique to censor biological echoes in radar reflectivity data," *J. Applied Meteorology*, vol. 49, pp. 435–462, 3 2010.

[13] M. Sezgin and B. Sankur, "Survey over image thresholding techniques and quantitative performance evaluation," *J. of Electronic Imaging*, vol. 13, no. 1, pp. 146–165, 2003.

[14] N. Otsu, "A threshold selection method from gray-level histograms," *IEEE Trans. Sys., Man., Cyber.*, vol. 9, pp. 62–66, 1979.

[15] R. Delanoy and S. W. Troxel, "Machine intelligent gust front detection," *The Lincoln Laboratory Journal*, vol. 6, pp. 187–212, 1993.

[16] J. Johnson, P. MacKeen, A. Witt, E. Mitchell, G. Stumpf, M. Eilts, and K. Thomas, "The storm cell identification and tracking algorithm: An enhanced WSR-88D algorithm," *Weather and Forecasting*, vol. 13, pp. 263–276, June 1998.

[17] V. Lakshmanan, "A separable filter for directional smoothing," *IEEE Geosc. and Remote Sensing Letters*, vol. 1, pp. 192–195, 7 2004.

[18] D. Charalampidis, T. Kasparis, and W. Jones, "Removal of nonprecipitation echoes in weather radar using multifractals and intensity," *IEEE Trans. Geosci. Remote Sensing*, vol. 40, pp. 1121–1132, 2002.

[19] E. Anagnostou, "A convective/stratiform precipitation classification algorithm for volume scanning weather radar observations," *Meteorol. Appl.*, vol. 11, pp. 291–300, 2004.

[20] J. Blum and J. Rosenblat, *Probability and Statistics.* Philadelphia: W.B. Saunders Company, 1972.

[21] J. Zhang, K. Howard, S. Vasiloff, C. Langston, B. Kaney, A. Arthur, S. Van Cooten, K. Kelleher, D. Kitzmiller, F. Ding, D. Seo, M. Mullusky, E. Wells, T. Schneider, and C. Dempsey, "National mosaic and multi-sensor QPE (NMQ) system: description, results and future plans," in *34th Conference on Radar meterology*, (Williamsburg, VA), p. 7A.1, Amer. Meteor. Soc., 2009.

[22] V. Lakshmanan, T. Smith, G. J. Stumpf, and K. Hondl, "The warning decision support system – integrated information," *Weather and Forecasting*, vol. 22, no. 3, pp. 596–612, 2007.

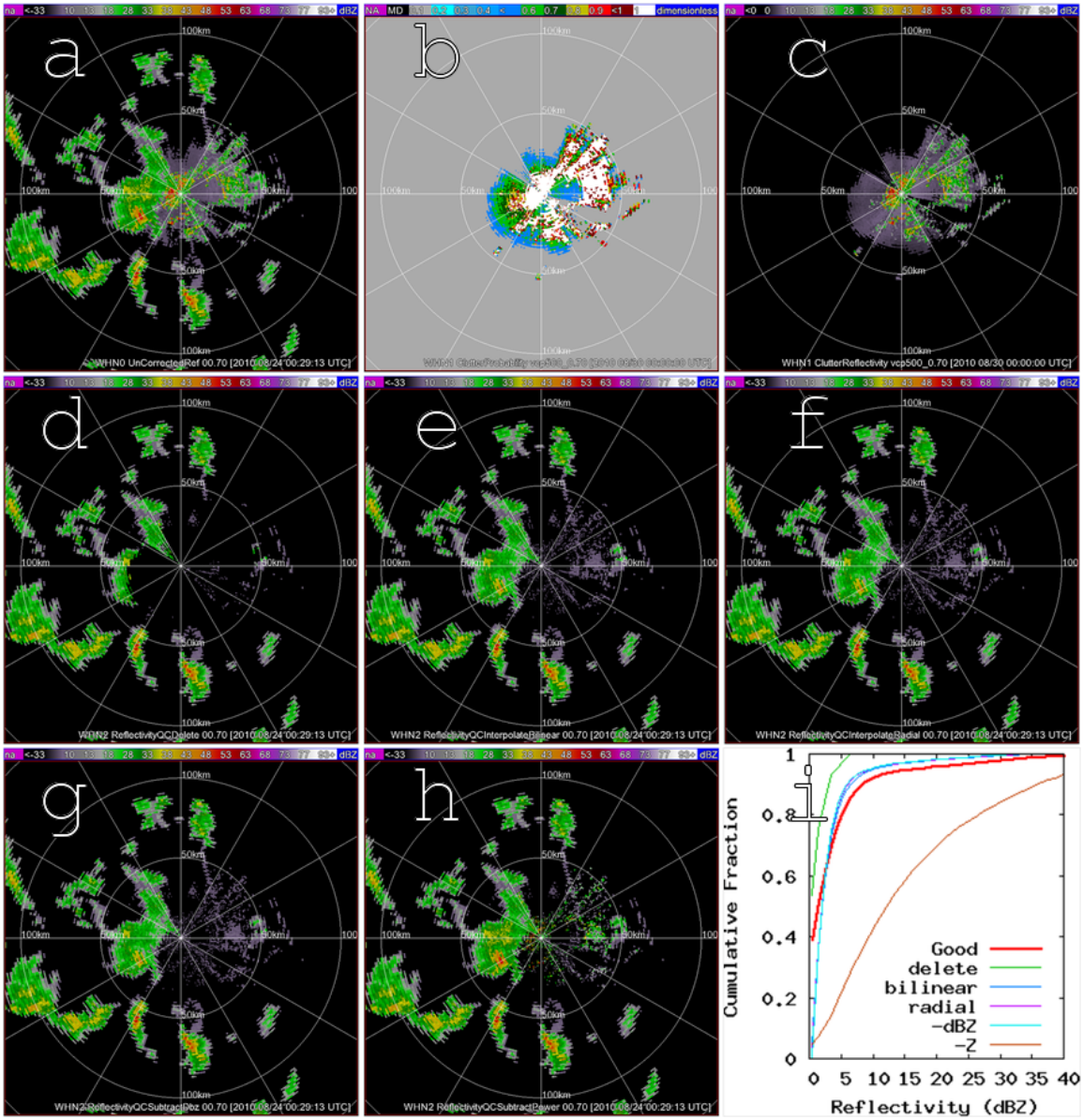

Fig. 2. (a) Uncorrected reflectivity collected at an elevation of 0.70 degrees by the Jimmy Lake, Alberta (WHN) radar on Aug. 24, 2010; (b) probability of persistent clutter derived from 1 day of data from WHN; (c) estimate of the reflectivity of persistent clutter. (d) Simply deleting the reflectivity data at clutter locations; (e) Bi-linear interpolation to fill clutter locations; (f) Interpolation along radials; (g) Subtracting dBZ value of clutter; (h) Subtracting Z value of clutter; (i) Quantitative evaluation of the clutter mitigation methods shown in panels d-h using the Kolmogorov-Smirnov test. The distribution of the bi-linearly interpolated pixels is nearly identical to the distribution of good pixels.

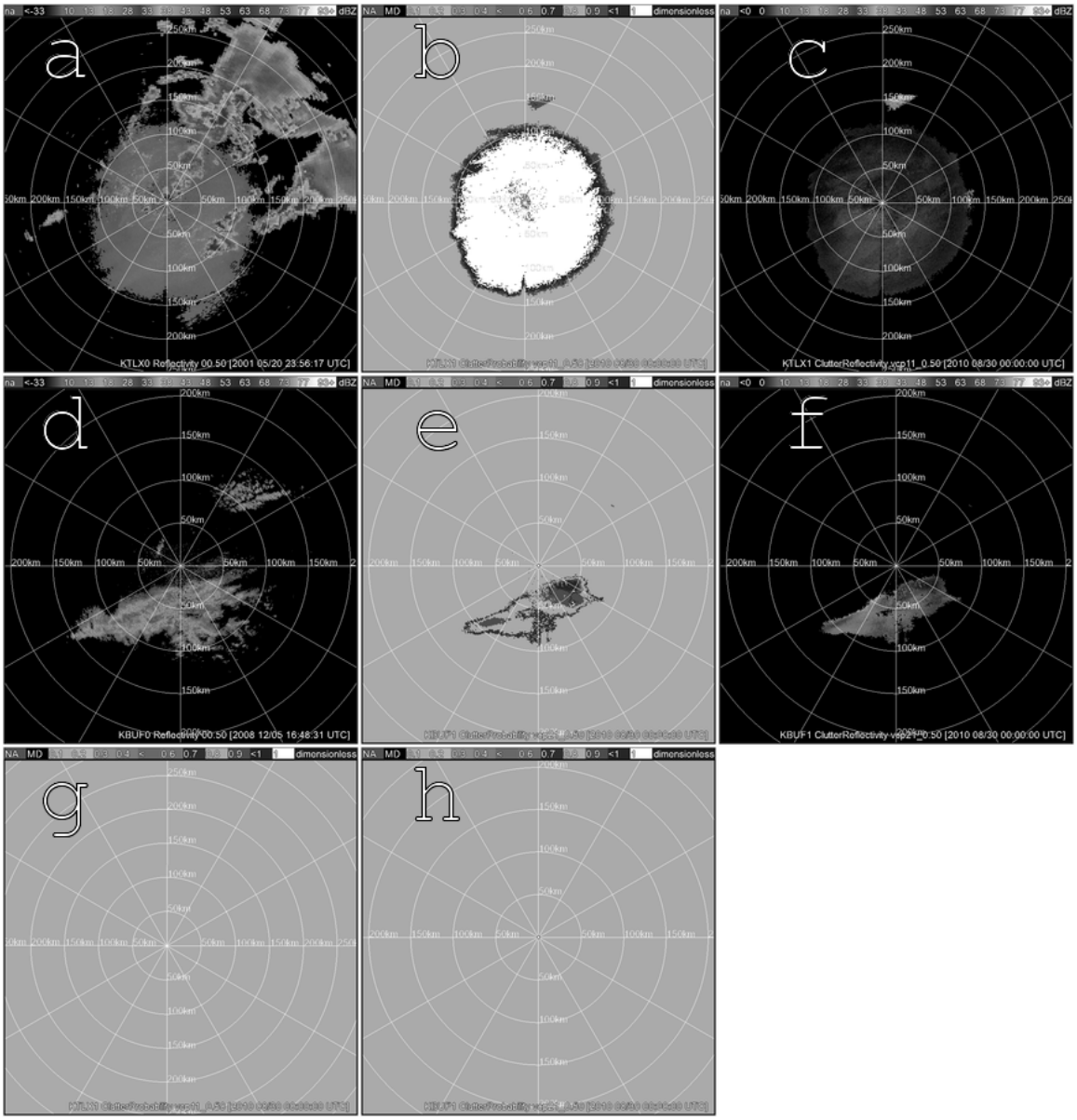

Fig. 3. The clutter removal technique based on just reflectivity does not work well on small datasets with biological echoes or with stationary, long-lived systems such as lake-effect snow. However, incorporating Doppler velocity data addresses both these issues. (a) Data from Oklahoma City, OK on May 20, 2001; (b) the areas identified as clutter include the areas where biological echoes persisted the entire duration; (c) the "clutter" reflectivity are low values, so a subtraction correction strategy will have less impact than an interpolation one. (d) Data from Buffalo, NY on Dec 5, 2008; (e) lake effect snow is misidentified as clutter (f) the clutter reflectivity pertains to the snow; (g) Clutter reflectivity from the Oklahoma City case in the top row when Doppler velocity is also used to identify clutter pixels; (h) Clutter reflectivity from the Buffalo case in the middle row when Doppler velocity is used in clutter identification;

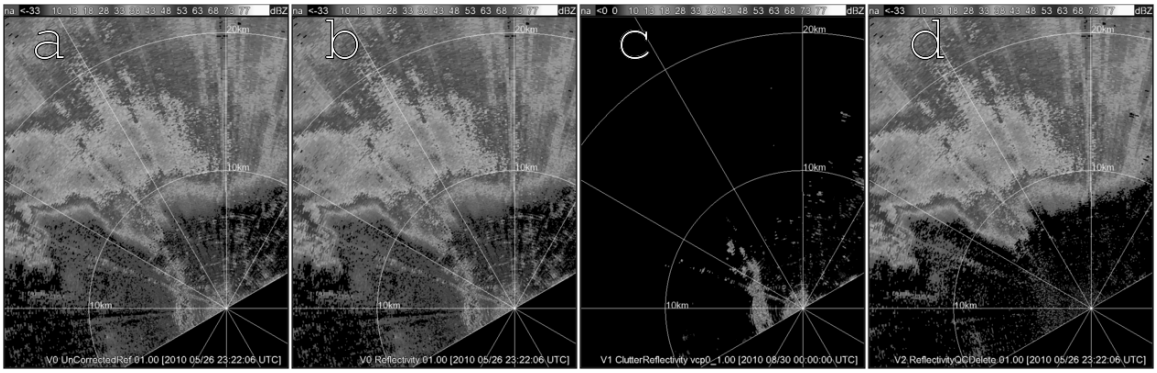

Fig. 4. The clutter removal technique can be applied to mobile radar data. (a) Reflectivity; (b) Reflectivity corrected by the signal processor continues to show the impact of ground clutter; (c) Clutter reflectivity derived statistically from about 90 minutes of reflectivity and velocity data; (d) Clutter-mitigated reflectivity shows the ground clutter removed.

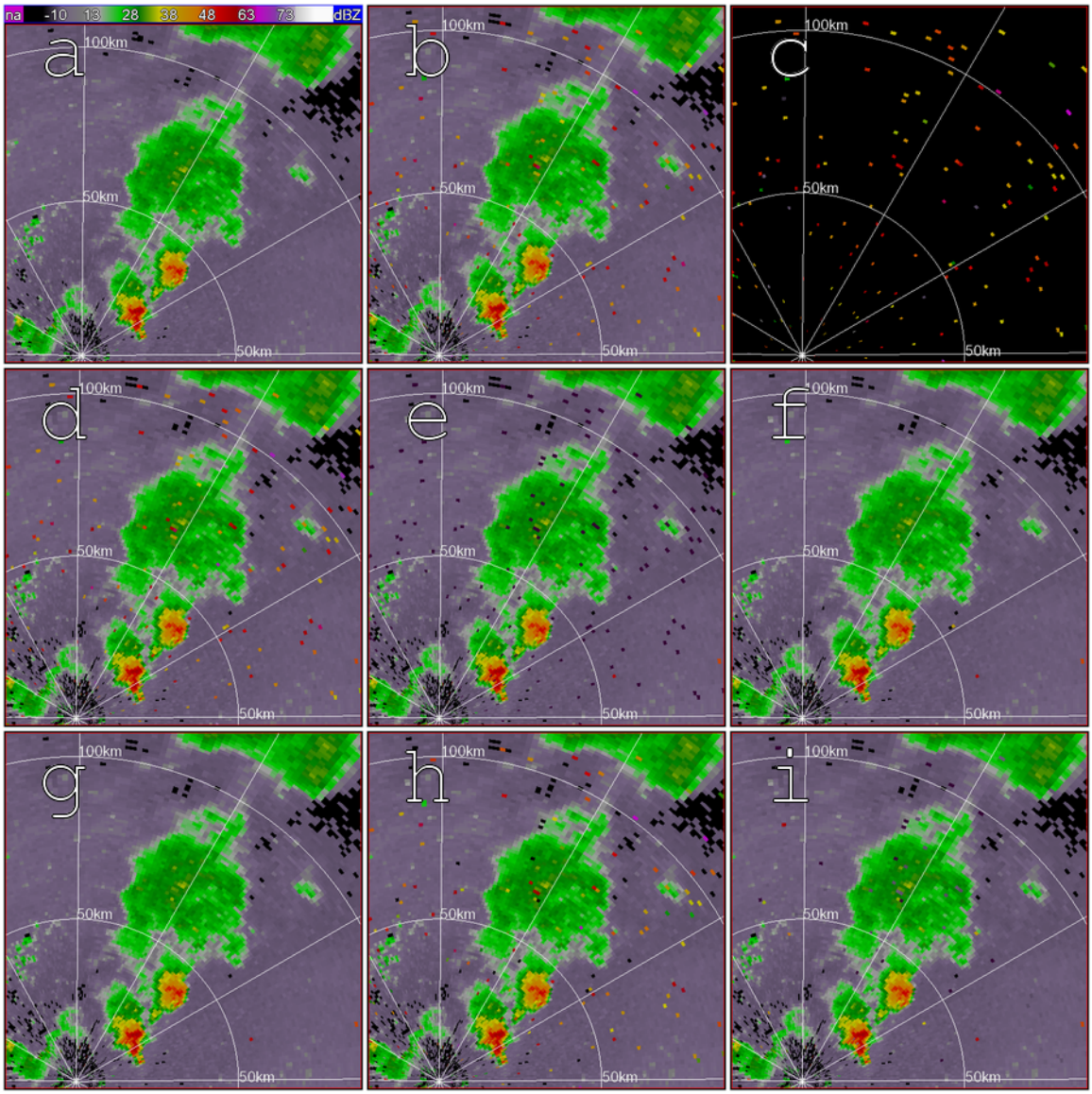

Fig. 5. Adding simulated clutter to real reflectivity data and using the technique of this paper to mitigate its impact. (a) Original reflectivity data from the Oklahoma City NEXRAD on May 20, 2001. (b) Clutter simulated at p of 0.01 and added to the data. (c) Clutter reflectivity identified using the technique of this paper. (d) The automated quality control of [9] without clutter mitigation applied to the data in (b). (e) Clutter pixels identified from (b) and deleted. (f) Same as e, but mitigated by interpolating along radial. (g) Same as e, but using bi-linear interpolation. (h) Same as e, but subtracting Z. (i) Same as e, but subtracting dBZ.

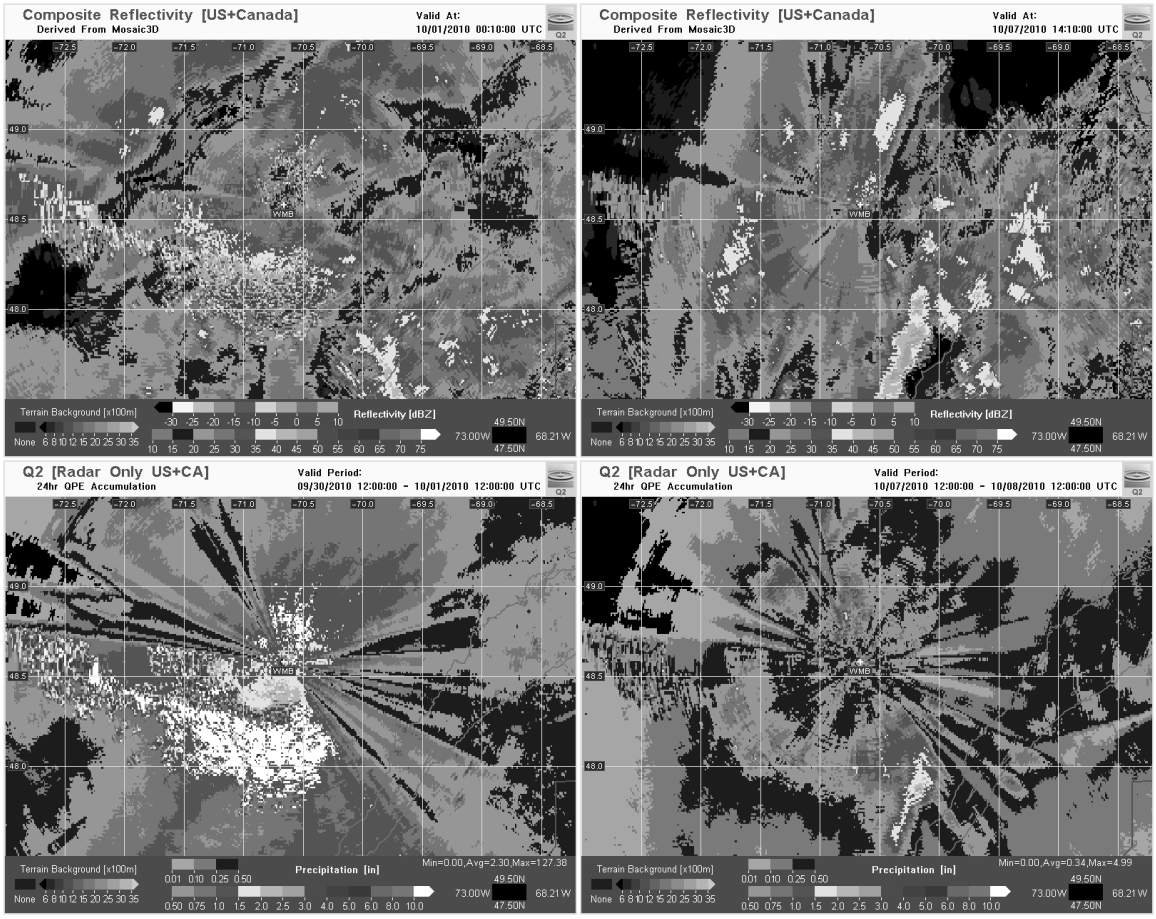

Fig. 6. Impact of applying the statistical clutter map in real-time. Left: Composite reflectivity (top) and 24-hour precipitation accumulation (bottom) from the WMB radar on Oct. 1, 2010 before the application of clutter map. Right: Composite reflectivity (top) and 24-hour precipitation accumulation (bottom) from the WMB radar on Oct. 7-8, 2010 after the application of clutter map.